

## Experimental Trials of Pre-Casted Column/Beam Connection for Cyclic Loads

Tiago André Pacheco de Almeida

---

**Abstract:** Construction joints in precast structures are inevitable and it must ensure suitable performance to the structure, ideally with structural continuity. This is important for the response to vertical actions and the actions with seismic origin, to obtain an equivalent performance to a fully concreted structure "in situ".

Following experimental research which analyzed the behavior of these joints next to the areas of beam/beam connections, this work presents the experimental results and their interpretation of analyses for cyclic loading simulation of seismic effects, for that kind of positioned joints for a beam/column connection.

With these tests it was intended to extend the scope of previous works for monotonic actions to the situation of cyclical actions. Interpreting the results of the tests, it can be concluded that the structural response is only marginally affected of joints with different age concretes. These findings were evaluated in experiments in which the connection characteristics of the concrete surface were roughened particularly low.

Beyond the detailed analysis of the characteristics of the behavior of these near joints, it is called attention to the potential design of construction processes with precast elements in the connection joints may be provided in areas of high stress (bending and/or shear). Indeed it is concluded, in general, that this type of connection provides overall service behavior characteristics and resistance, very close to the continuous reinforced concrete. Even in terms of ductility, characteristics are not seriously affected.

**Keywords:** Precast concrete, column/beam connection, cyclic test, construction joints, structural continuity, seismic Behavior

---

## 1 Introduction

### 1.1 Objectives and Methodology

In this paper we study one concrete beam-column connection subjected to cyclic loading in order to assess their performance. The objective is to understand how the presence of joints disturbs the normal operation of the connecting node. Through cyclical actions we intend to investigate how the strength and ductility of the connections are affected under this type of loading.

### 1.2 General Framework

The prefabrication of structures appears in order to industrialize the building. The construction of buildings shall be formed by isolated components that bind in site-building. These components are only products manufactured on assembly lines in factories (Santos, 1983), resembling the industry in general. In precasting, connections are natural areas of the structure and are developed at the implantation site of the work in very different conditions of the remaining structure. This aim to

repay the monolith that is seen in monolithic structures (Proença, 1996). The biggest disadvantage is the difficulty in creating links between the various elements without being detrimental to the overall functioning of the structure. In order to establish a compromise between structurally efficient solutions in precast structures, it is necessary to study its biggest "weakness", the links between the structural elements subjected to seismic action.

## 2 Precast Column/Beam Connection Investigation

Cavaco (2005), "Construction Joints Between Precast Elements". This work is rehearsed four beams to failure for monotonic loading. Two reference beams ( $V_{1ref}$  and  $V_{2ref}$ ) without construction joints and two precast beams ( $V_{1P}$  and  $V_{2P}$ ). In  $V_1$  group beams had a lower number of transverse reinforcement in order to cause a shear failure and check how it could affect this type of situation. In  $V_2$  group beams had higher amount of

transverse reinforcement, looking for the breakup of that by bending moment and high shear in the web. With the V1 test group was observed that the presence of the joint in no way interferes because in both cases it is fragile failure by shear. This failure is undesirable but is already known by the reinforced concrete structures. In the V<sub>2</sub> test group is concluded that the resistant capacity of the beams was identical, however it has been found in precast beam a lower ductility behavior.

Pacheco (2007), "Behavior of connections in concrete between precast parts". This work builds on the work of Cavaco (2005). Four types of beams were tested. At V<sub>1</sub> beam was applied two different types of structural adhesive joints interface. V<sub>2</sub> and V<sub>4</sub> beams follow on from previous work but with the inclusion of longitudinal reinforcement crossing the joint. The V<sub>4</sub> had a lower rate of longitudinal tension reinforcement that the V<sub>2</sub>, which is the criterion for differentiation. The planned ductility of the beam V<sub>2</sub>, face to the V<sub>4</sub> beam was lower, a situation that was confirmed later. V<sub>3</sub> beam intended to show the effect of inclined joint in two different directions. After the tests conducted it was possible to draw the following conclusions: (i) Even in the presence of structural glues, the joint interface still produces an earlier crack in the zone and no improvement in performance; (ii) the extra reinforced bars in the web allows an improvement in ductility and crack scheme, situations resemble a monolithic connection. (iii) Whatever the inclination of the inclined joint studied, in both situations the resistant capacity was not affected, the cracking was due to "normal" and the ductility was very similar to a monolithic connection.

Gião (2012), "High Seismic Performance Beam-Column Connection". This research focused on the study of the seismic behavior of a beam-column connection. The experimental study included analysis of the hysteretic behavior of the critical zone of the beam. According to the author, a reinforced concrete structure subjected to cyclic action, if the gravity loading is significant, the mechanism of failure may be associated with the formation of two unidirectional hinges on the beam - one close at the beam/column connection and the other on the span. The hinge deformation in the beam-column connection stops to be directly relatable to the imposed deformation on the pillar and becomes dependent on the plastic deformation of the span hinge. Thus, the present study implemented a cyclic test procedure that best simulates the actions that a beam is subject, i.e. to include the effects of horizontal loads acting simultaneously with the vertical loads. The results showed that for the study of hysteretic response of

beams with a significant level of gravity loads, the cyclic test procedure alternated with gravity loads seems more realistic than it takes no account of the gravity loads.

### 3 Experimental Model

#### 3.1 Model Geometry

According Gião (2012), for the analysis of a portico subjected to horizontal displacement and the vertical loads, for the purpose of defining the simplified model, it may correspond to a cantilever beam with a length of L/3. The model represents an edge beam, actual scale, set in a portico structure with a 4.5m span, which in view of the above analysis, the model is reduced to a cantilever beam with a 1.5m span (Figure 3.1).

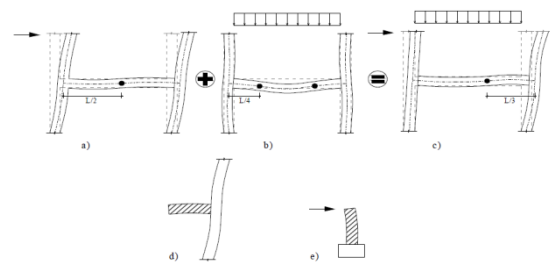


Figure 3.1 – Geometry Conception of experimental model (Gião, 2012)

To take into account the possible existence of high shear combined with bending moment, it was chosen for an "I" cross section, in order to strengthen the web and condition the same. Thus, it can get a geometrically identical beam to Gião (2012), but comparability with the work of Cavaco (2005) e Pacheco (2007) model. It was developed a 3D geometry by *SketchUp* drawing program in order to have a more realistic perception of the experimental model, as shown in Figure 3.2.

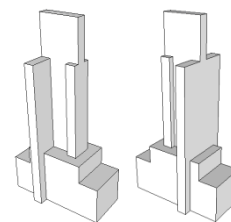


Figure 3.2 – 3D Model in vertical position (both sides view)

In Figure 3.3 it can be observed the 3D drawing of isolated beams, i.e., after the first phase of concreting, as well the difference in the types of inclination joints at the described models.

The experimental campaign can be summarized in the Table 3.1.

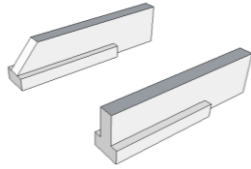


Figure 3.3 – 3D drawing for the first phase of beams

Table 3.1 Experimental campaign

| Model   | Joint    | Web extra reinforcement | Trial              |
|---------|----------|-------------------------|--------------------|
| V1 Beam | Vertical | No                      | Alternating Cyclic |
| V2 Beam | Vertical | Yes                     | Alternating Cyclic |
| V3 Beam | Inclined | No                      | Alternating Cyclic |
| V4 Beam | Vertical | No                      | Vertical Loads     |

### 3.2 Model Resistant Capacity

In the following table lies the ultimate capacity in terms of bending moment and force applied, evaluated based on mean values of materials resistance.

Table 3.2 – Beams ultimate capacity

| Beam | Bending Moment | $M_r$ (kN.m) | $P_u$ (kN) |
|------|----------------|--------------|------------|
| V1   | -              | 312          | 208        |
|      | +              | 167          | 111        |
| V2   | -              | 314          | 209        |
|      | +              | 167          | 112        |
| V3   | -              | 313          | 209        |
|      | +              | 167          | 111        |
| V4   | -              | 313          | 209        |
|      | +              | 167          | 111        |

The ultimate force ( $P_u$ ) is the result of the bending moment ( $M_r$ ) divided by beam length since the connection zone to the actuator (1.5m).

## 4 Experimental Program

### 4.1 Trial System

The beam is tested in a vertical position to facilitate assembly and testing. On top of the beam is placed a head of metal profiles connected to a mechanical actuator, it is coupled to a reaction wall resting on the slab. Between the beam and the head of the actuator there is a monitoring system comprises a load cell of traction-compression and displacement transducer. The

Figure 4.1 illustrates the scheme used in the laboratory test.

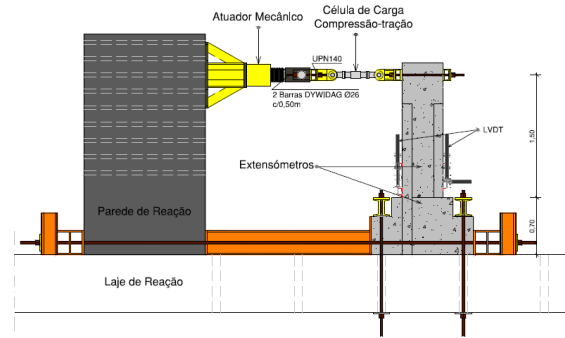


Figure 4.1 – Trial System Scheme

### 4.2 Test Procedure

We opted for the realization of quasi-static tests. The balance equation that translates equality between these forces is the follow:

$$k_u = F(t) \quad (4.1)$$

Thus, the quasi-static tests allow obtaining the refund system forces and the observation of inelastic behavior.

#### 4.2.1 Alternating cyclic test

The first protocol is the imposition of a story of cyclic and alternated with increasing displacement amplitude, including a repetition of three cycles with the same displacement amplitude ( $\Delta$ ), as illustrated in Figure 4.2. The story shifts to be applied was  $\pm 0,5\Delta$ ,  $\pm 1,0\Delta$ ,  $\pm 2,0\Delta$ ,  $\pm 3,0\Delta$ ,  $\pm 4,0\Delta$ ,  $\pm 5,0\Delta$ ,  $\pm 6,0\Delta$  and  $\pm 7,0\Delta$  with three cycles of equal amplitude.

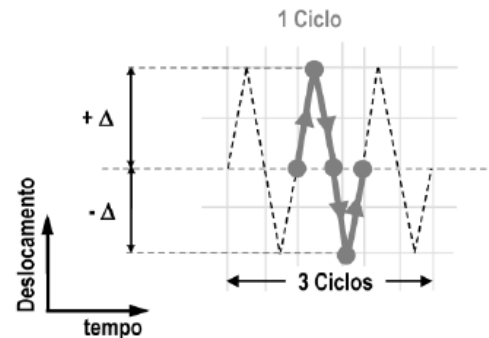


Figure 4.2 – Displacement imposition for alternating cyclic test (Gião, 2012)

It was established as the criterion for failure of the trial the moment it reached 85% of maximum force criterion also used by Gião (2012) supported by the consulted references.

#### 4.2.2 Cyclic test with gravity loads

This protocol, which was used in  $V_4$  beam, constitutes a story of application of alternating amplitudes with increasing displacement from the effects of the gravitational load. I.e., the imposition of the displacement cycle is felt from the moment

the pre-set value of the gravitational load is restored. This procedure involves the completion of the controlled trial by force and displacement.

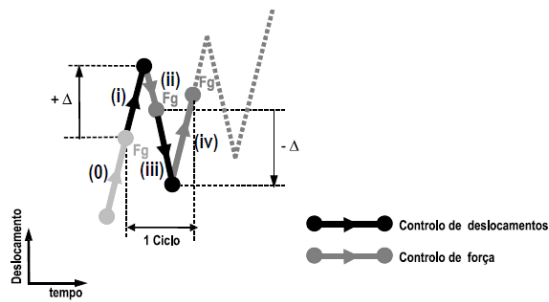


Figure 4.3 – Displacement imposition for cyclic test with vertical loads (Gião, 2012)

The imposed displacements (Figure 4.3) are the same as above protocol, but with the particularity of each cycle having a different starting point due to the gravitational load restoring that occurs for successively larger displacements. Failure occurs when the connection is unable to resist the vertical forces.

### 4.3 Experimental Results

The reference displacement ( $\Delta$ ) imposed was 6mm and the story shifts already mentioned in the protocol. Positive displacements correspond to displacements in the direction of the beam negative moment. Figure 4.4 represents the displacement diagram of the story shifts occurred during the  $V_1$  beam test.

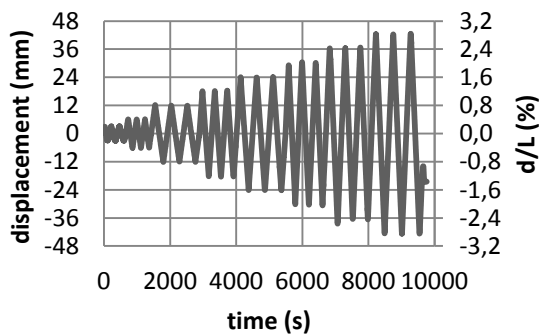


Figure 4.4 – Imposed displacement diagram of V1 test

The resulting diagram of the test characterized by a non-symmetrical hysteresis diagram as can be seen in Figure 4.5. By graphical observation, the resistant capacity of the beam is different in both directions and it meets the estimated analytically. The maximum force for negative moments was 212,6kN and it was reached in the first cycle corresponding to 30mm ( $5,0\Delta$ ), while the maximum moment for positive force was 113.32kN at the first cycle of 18mm ( $3,0\Delta$ ). The yield in the direction of negative moments occurred for a displacement of 24mm ( $4,0\Delta$ ) and in the other half, a displacement of 12mm ( $2,0\Delta$ ). While already a

direction enters the post-yield scheme, the other is still in the elastic phase. In the direction of positive moments, cycle after cycle, post-yield stiffness is more pronounced than in the other direction. In the initial phase ( $d = 3\text{mm}$ ) the stiffness is very similar in both directions. At  $d=6\text{mm}$ , in a positive direction when the stiffness is slightly less, as would be expected.

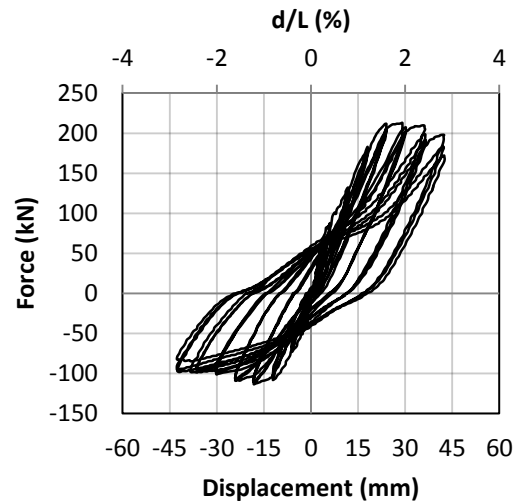


Figure 4.5 – Force-displacement diagram of V1 test

The first cracks appear soon shifts to 3mm. However, for these negative moments mainly affect the slab while the other direction, the cracks extend beyond the bottom flange also appearing at the web area. For negative moment, the cracks only arrive at the web for displacements of 6mm. In the first cycle, cracking occurs in normal shape, however it is noted disturbance in cracking due to the presence of the joint, i.e. cracks tend to change trajectory in the presence of the joint. When more advanced cycles ( $4,0\Delta$ ,  $d=24\text{mm}$ ) was reached, it was possible to observe the perturbation of the crack. In Figure 4.6 there is a crack that coming to the joint deflects the trajectory tracking the joint.

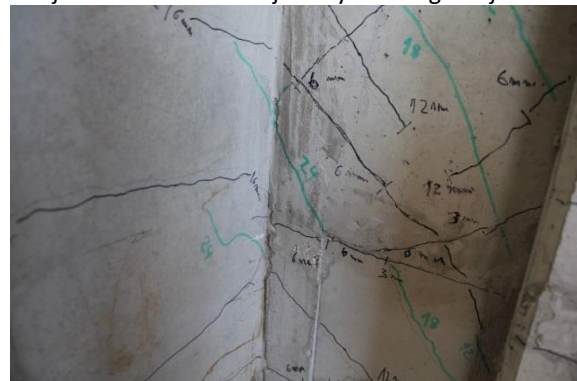


Figure 4.6 – Cracking at advanced cycle (V1)

The bottom flange of the beam was very sacrificed. The  $\varnothing 8$  bars start buckling after compression in the

3rd cycle of  $6,0\Delta$ ). In early  $7,0\Delta$  is notorious the destruction of the bottom flange and then we started to loss beam resistant capacity. In the direction of positive moments, the  $\varnothing 8$  bars reached the failure at the end of the last cycle. The test ended when the load capacity of the beam has fallen to about 180kN (approximately 85% of maximum) in the direction of negative moment. In we observe the final aspect of the connection after removing the damaged area of the compressed concrete. This damage was occurred for negative moments.



Figure 4.7 – Final aspect of connection (V1)

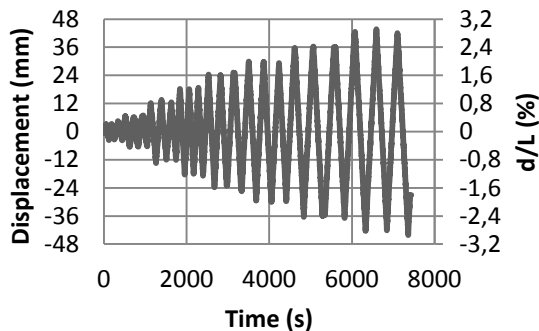


Figure 4.8 – Imposed displacement diagram of V2 beam

V2 beam followed the same procedure as V1 beam. The V2 beam had the longitudinal reinforcement in the web. The Figure 4.8 shows the displacement-force diagram imposed over time. This beam had a very similar behavior to the previous beam. Regarding the resistant capacity is noted a slight increase from the previous beam in both directions. To the direction of negative moment the maximum force occurred on the same displacement of the anterior beam ( $d=30\text{mm}$ ) and it was 233,8kN. For the positive moment the maximum force was 120,8kN also to the displacement of 18mm ( $3,0\Delta$ ). By observation of the resistant capacity of this beam was slightly higher. The post-yield stiffness and ductility are very similar to the previous one. The maximum

displacements were identical just like the levels of drift ( $d/L$ ).

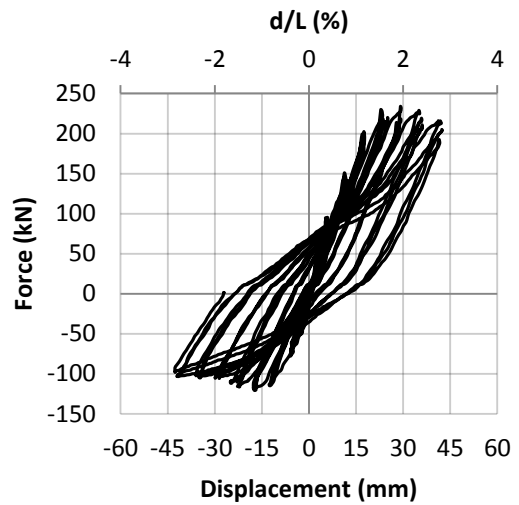


Figure 4.9 – Force-displacement diagram of V2 test

Regarding the distribution of cracking is observed that the cracks progress continues to be disturbed by the presence of the joint. However we note a slight improvement on the V1 beam. The initial cracking scheme is very similar to that of V1 beam. For positive moments the flange and the web crack to displacements of 3 to 6mm, while the other direction has the same pattern but for displacements of 6 and 12mm. Just like the previous one, at the end of cycles  $6,0\Delta$  there shucking the material covering the bottom flange and the end of  $7,0\Delta$  there is the destruction of the bottom flange and buckling of  $\varnothing 8$  bars. There was no rupture of the bars. The test was terminated at the last cycle of the displacement  $d=42\text{mm}$  when the maximum force only achieved 187kN in the direction of negative moment. At the end of the test we notice that the connection behavior was very similar to the above.

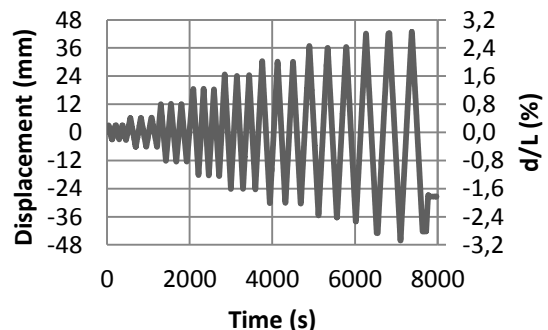


Figure 4.10 – Imposed displacement diagram of V3

V3 beam was tested with same protocol as the previous ones In Figure 4.10 is the force-displacement diagram of this test.

In terms of ductility and resistant capacity, this are to the same level as the first beam as shown in Figure 4.11. The maximum forces were 212,4kN for 24mm in negative moment and 115,0kN for a displacement of 18mm in the other direction. This time, cracks appear to follow a current distribution. The parallel slits parallel to the joint and the perpendicular cross the joint without problem.

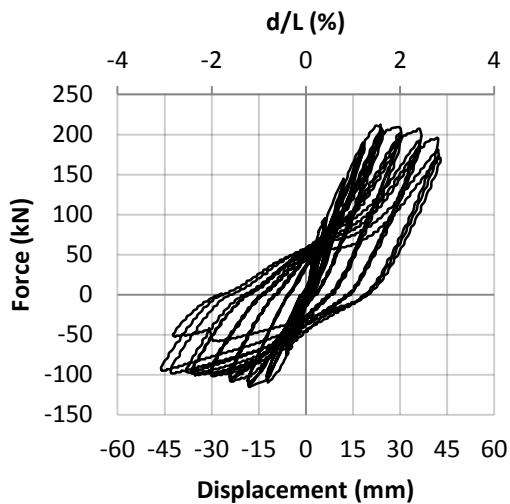


Figure 4.11- Force-displacement diagram of V3

In advanced cycles, cracking continues in the same pattern of a monolithic beam. The peel of the covering on the bottom flange occurred in the 3rd cycle of 5,0Δ and the buckling of ø8 bars to. The more premature peeling made in cycles d=36mm, the bottom flange was heavily damaged. So, the 1st cycle of 7,0Δ existed buckling of ø16 bars towards negative moments. At this stage the beam began to lose capacity and the last cycle, there was a failure of ø16 bar by traction in the direction of positive moment. This phenomenon can be seen in the graph force-displacement when the load capacity in the direction of positive moments does not go more than 50kN in the last cycle. It is evident the destruction of the bottom flange and the buckling of the ø8 bars.

The V4 beam is completely identical to V1 beam, except in the protocol for imposition of deformation during the test. The procedure consisted of applying a pre-established vertical load equivalent to the gravitational load, which was estimated as the value of 90kN. The imposed displacements were equal of the other tests. In Figure 4.12 can be observed the force-displacement diagram over the time. The offsets for negative moments in this diagram have negative sign. You may notice a significant difference in the progress of graphics. In the diagram it can be seen an cycle alternately

displacement around an initial displacement (displacement due to gravity load). This behavior occurs for the first two cycles of full load (6 replications). After the yeild for negative moments, the beam starts to get a permanent deformation in that direction (without recovery).

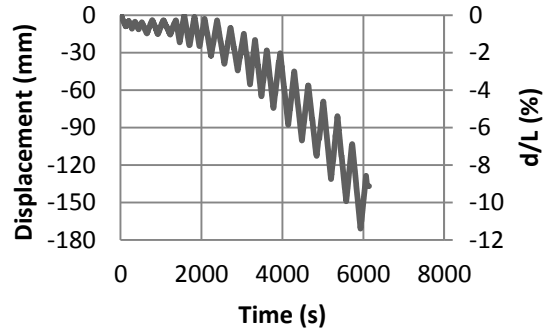


Figure 4.12 – Imposed displacements for V4 test

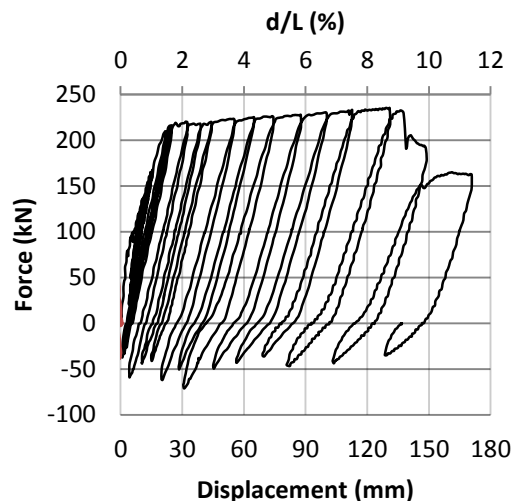


Figure 4.13 – Force-displacement diagram for V4 test

The maximum force achieved for negative moments were 235,4kN and occurred for the 1st cycle of 6,0Δ displacement. The maximum force for positive moments was 71,1kN, i.e. the yeild was not achieved in this direction. In terms of ductility and compared with three other trials with another protocol, there is a substantial improvement. It can be observed in the force-displacement diagram shown in Figure 4.13, that the imposition of the procedure test produces a clearly different hysteretic behavior. There is an amplification of the deformation phenomena observed in relation to alternating cyclic test. When applied force corresponding to the gravitational force of 90kN, this generates an displacement of 5,78mm, so that there is crack in the slab at the web area. In the first cycles, the cracking occurs exclusively in the

direction for negative moments. The bottom flange seems to suffer less wear than in previous beams (because there is no transfer for traction). The cracks pass through the joint as if it did not exist. In more advanced cycles, the bars also end up, presenting due to the massive deformation, high buckling phenomena. In the 2nd cycle of 6,0Δ, beam has significant damage to the bottom flange and starts to lose capacity. The assay was terminated at the end of the 3rd cycle for that displacement. In Figure 4.14 it is possible to observe the accumulated deformation in the direction of negative moments at the end of the test.



Figure 4.14 – Final deformation of V4 beam

## 5 Results Interpretation

### 5.1 Cracking

With the V1 beam intended to be a direct comparison with the monotonic models of previous works and therefore the comparison with the monolithic model tested now the cyclical loads.

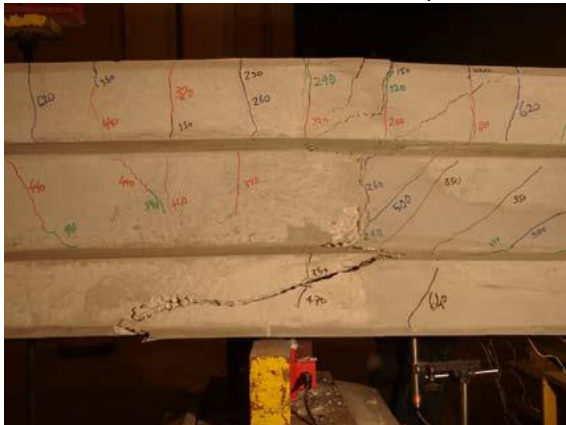


Figure 5.1 – Path of loads (Cavaco, 2005)

Starting by comparison with monotonic models, the beam begins by presenting a scheme very similar to the cracking seen in other works. The

presence of the joint disturb the way of loads concentrating the compressive stress in the lower flange (Figure 5.1), which finally results in failure with ductility loss (Cavaco, 2005). In these trials, although the two flanges are compressed alternately as the lower flange section area is less; it is understandable that for the same level of this shift this is the most affected (Figure 5.2). In the area of the slab there is no vertical joint. This fact is favorable because do not exist a weakened area that contributes to form a vertical joint in the slab. For comparison with the test of cyclic action (Gião, 2012) it is verified that the cracking and its distribution are similar.

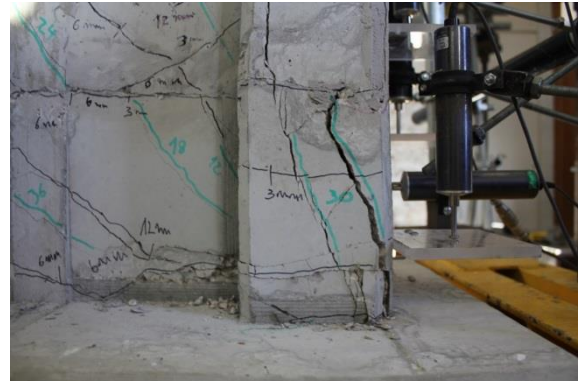


Figure 5.2 – Peel the lower flange (V1)

With V2 beam, we wanted to understand how the web longitudinal reinforcement could improve the behavior for the same cycling tests. It is noted that the monotonic testing for this type of solution has proved particularly satisfactory. In this test the initial crack was identical scheme with no expected differences. In a interface joint resistance is influenced by the bolt effect, the aggregates interlocking and the surface treatment.



Figure 5.3 – Final cracking of V2 beam

In this test the board did not take any special treatment and was having a substantially smooth interface, so as to become the most unfavorable

situation. It is believed that this aspect has no apparent effect on the improvement of crack distribution along the joint.



Figure 5.4 – Final cracking of V3 beam

In studies of monotonic tests (Cavaco, 2005) (Pacheco, 2007), the inclined joints were shown to be a good solution when placed either perpendicular or parallel to the expected cracks. We analyzed only one inclined joint on more practical direction to run at work. The cracking, on V3 beam (Figure 5.4) was identical to the monotonic. The fact that the joint is in the same direction of the cracks for negative moment is causes the crack is formed earlier, because this area is more fragile. The joint can be understood as causing an early crack, which turns out to hardly affect the behavior at failure.



Figure 5.5 – Final cracking at V4 beam

The V4 beam placed in test the protocol more recently proposed in the literature and laboratory practice to analyze the effects of the seismic action. With this protocol, it had become a closer behavior that we can find at the nodes in a structure subjected to an earthquake. The beam

deforming mainly in one direction (negative moment). With this protocol in which the behavior is leading to negative moment, there are two favorable facts namely: (i) the vertical crack in the web do not formed because the slab by failing joint caused the cracks appear in other sections having been formed an inclined crack in the soul regardless of the existence of the joint (Figure 5.5); (ii) the failure to verify alternating traction yield of reinforced bars and high compressions bottom flange increases very significantly the ductility for negative moments.

## 5.2 Global Behavior

The overall behavior of the V1 beam against the models used as reference proved quite satisfactory. The resistance achieved was estimated analytically, as previously mentioned. The stiffness remains linear until the yield, the time from which it will degrade cycle after cycle. The overall behavior is similar to a monolithic beam. In terms of overall behavior of V2 beam, there was a small increase in resistance capacity, however improvement in ductility. It may be noted that the web longitudinal reinforcement improves the behavior of the beam, although in this test this conclusion can not be enhanced. In Figure 5.6 are shown curvatures associated with the yield moments and the curvatures envelope in both directions. The positive sign corresponds to the positive moment and for the other direction is the same. The diagrams presented some "spikes", this is due to the fact that the readings are discrete and not continuous along the beam. However, the diagrams show the same movements, such as seen in the force-displacement diagram.

Regarding the analysis of the beam V3, compared to V1 beam, the behaviors are very similar, however we highlight some aspects. The resistant capacity of both beams is of the same order of magnitude, and the initial stiffness. As for the post-yield stiffness in the more advanced cycles, is known to lose more abrupt stiffness of the V3 beam due to the V1 beam. This difference is due to the destruction of the V3 beam bottom flange previously contemplated. In V3 beam was failure of  $\phi 16$  bar towards positive moments. Regarding the curvature diagram (Figure 5.7) the maximum curvature envelope is very similar, if only highlights the fact that the peeling of the concrete cover have occurred earlier in the V3 beam and thus the reading in this diagram does not identify the maximum curvature in the nearest zone of restraint. The main difference lies in the yield curvature, since they have a higher value. There was a better connection performance during the



elastic phase, which had already taken place by cracking good scheme presented.

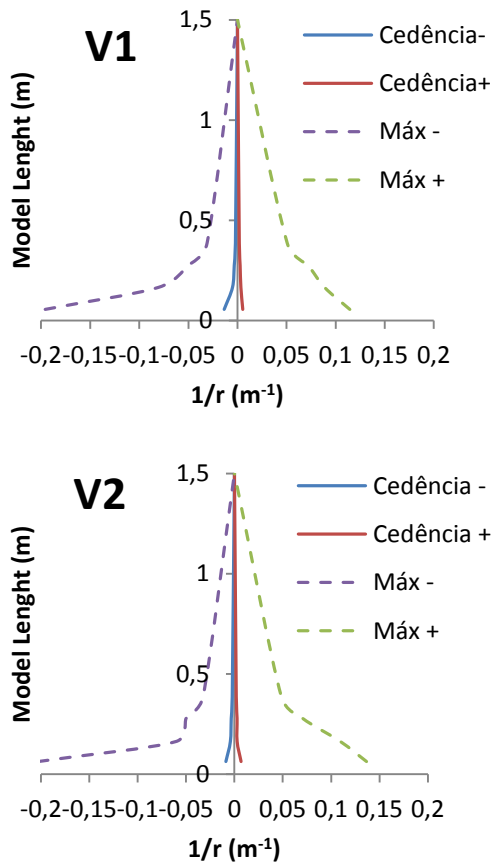


Figure 5.6 – Curvature diagrams for V1 and V2 beams

V3 beam was the only beam to present a more pronounced zone of fracture outside the joint area, i.e., closer to a restraint zone. As shown in Figure 5.8, in the direction of negative moments, opened a perpendicular crack to the joint and in the other direction it opened a parallel crack to the joint. This phenomenon possibly occurred because during the elastic phase beam behaved as a monolithic beam.

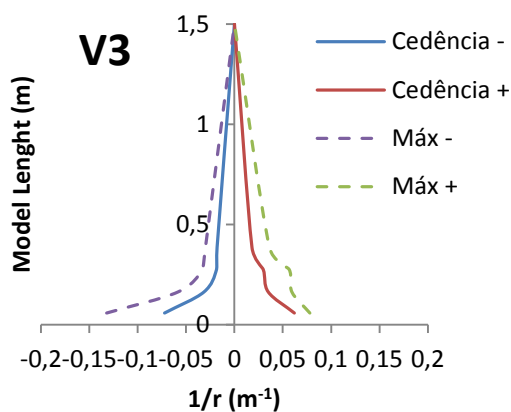


Figure 5.7 – Curvature diagram of V3 beam

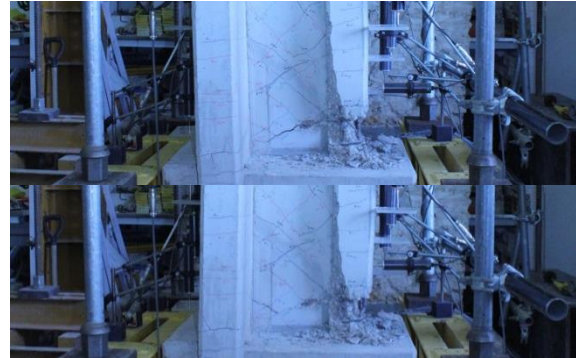


Figure 5.8 – V3 beam failure

With this protocol (V4 beam) in which the behavior is leading to negative moment, the fact that there would be alternating traction yield of reinforced bars and high compressions bottom flange increases very significantly the ductility for negative moments. Compared with the reference beam for this protocol, the performance of this beam was good. Ductility is identical to the reference beam and the levels of *drift* (ratio between the vertical displacement and the distance to the inflection point of the deformed beam, 1.5m). In this beam the progress of the curvature diagram (Figure 5.9) includes only the direction for negative moments, as there is an accumulation of deformation in this direction. Also note that the "linear" progress to the first known section is much more evident than in V1 beam.

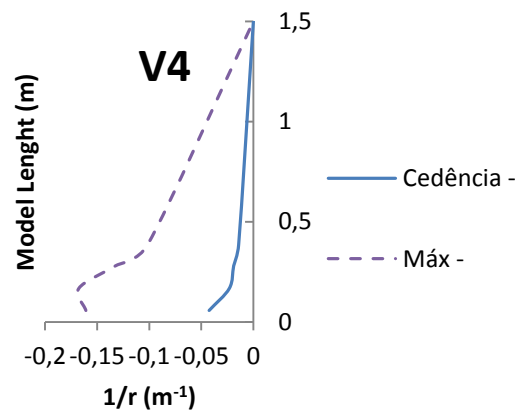


Figure 5.9 – Curvature diagram of V4 beam

## 6 Conclusion

The existence of a joint outside of the node zone has little negative impact on the overall performance of the structure. Compared with the reference models (Gião, 2012) it was possible to get a connection with the same kind of performance in terms of resistance capacity and ductility. A connection between different ages concretes the bolt effect combined with the aggregates interlocking, give the interface to its

ultimate capacity. The beam as it adopted more reinforced bars to cross the connecting joint, it has played a tough capacity slightly higher despite the predicted gains ductility were not evident in this test. Leads therefore to conclude that the use of reinforcement bar at the web interface certainly improves performance in terms of ductility as found in other tests. However in this test this conclusion can not be drawn up believing that the fact that the surface roughness was small has negatively affected the behavior. On the other hand the minimum reinforced bar to ensure this effect must be studied in more detail. The inclined joint may have positive effects, particularly in construction phase, which has more space to carry out concreting node. However the overall behavior was not much better than that observed in trials of vertical joints, which leads to the conclusion that constructive feature may be the deciding factor in choosing the solution in a particular case. Finally, the V4 beam tested with the protocol that takes into account the variation around the efforts of vertical loads, shows that precast connection with the slab to join the two pieces, resembles "almost" absolutely a connection monolithic. The protocol used in the first three beams, alternating cyclical, by it, did not show to be more appropriate for testing beams. These elements are subjected to vertical loads. If the test does not cover this type of loading, it happens that the beams enter yield phase for positive moments first, a situation that turns out to be very penalizing, because in the other direction when it reaches to yield phase the lower flange is already badly damaged. For this type of test, in which one wants to study the phenomenon of reversible hinges, the alternating cyclic protocol should be imposed from a displacement associated with the displacement of gravitational (or dead) loading. Thus, as can be seen in the example of Figure 6.1, a story of cyclic shifts alternating around a gravity displacement (6mm) causes the yield phase in both directions occur in the same cycle (24mm and 12mm, corresponding to beams of this paper). This will be expectable to have a good approximation of the of a reversible hinge behavior.

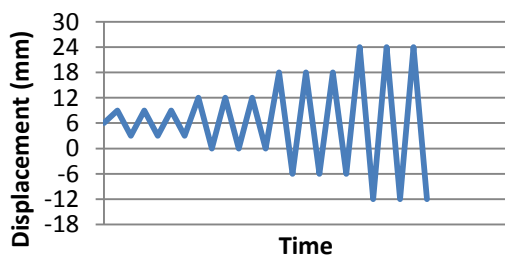


Figure 6.1 – Story shifts example

The protocol used in V4 beam, with contemplation of gravitational load, presents a good performance for unidirectional hinges connections. In fact, as it has already been studied previously, this protocol plays a good approximation for such connections. In short, it indicates that a good solution of precast connections can be made with vertical joint and web longitudinal reinforcements but with special care in the surface treatment giving it appropriate interface roughness. Anyway, the solution of an inclined joint may also be an appropriate solution to offer constructive advantages.

## 7 References

- Cavaco, E. (2005). *Juntas de Construção em Elementos Pré-Fabricados*. Dissertação de Mestrado em Engenharia de Estruturas, IST.
- Gião, A. R. (2012). *Ligação Viga-Pilar de Alto Desempenho Sísmico*. Tese para obtenção do Grau de Doutor em Engenharia Civil, Especialidade Estruturas, FCT, UNL.
- Pacheco, I. (2007). *Comportamento de Ligações em Betão entre Peças Pré-Fabricadas*. Dissertação de Mestrado em Engenharia de Estruturas, IST.
- Proença, J. M. (1996). *Comportamento Sísmico de Estruturas Pré-Fabricadas e Desenvolvimento de um Sistema Reticulado Contínuo*. Tese de Doutoramento, Instituto Superior Técnico, Universidade Técnica de Lisboa.
- Santos, S. (1983). *Comportamento de ligações de estruturas prefabricadas de betão*. Lisboa: LNEC Ed 57.